

# Dynamics of three coupled long Josephson junctions

Søren A. Hattel<sup>a</sup>, Anders Grunnet-Jepsen<sup>b</sup>,  
Mogens R. Samuelsen<sup>c</sup>

<sup>a</sup> *IRC in Superconductivity, Madingley Road, Cambridge CB3 0HE, United Kingdom*

<sup>b</sup> *Department of Chemistry and Biochemistry, University of California in San Diego, La Jolla, CA 92093-0340*

<sup>c</sup> *Physics Department, The Technical University of Denmark, DK-2800 Lyngby, Denmark*

Dynamics of a system of three long Josephson transmission lines coupled at a common end point is investigated. We report several periodic fluxon states and trace out the corresponding zero field steps. The boundary conditions at the common point lead to very different stability of steps for odd and even numbers of fluxons. In addition we find two “normal state” branches for the IV curve, where either two or three of the branches are in their normal state.

## 1 Introduction

Systems of stacked Josephson transmission lines have been studied recently both experimentally and theoretically [1,2]. Such systems may be relevant for that class of high temperature superconductors which are best described by the Lawrence-Doniach model [3,4]. In these materials (notably the thallium and bismuth compounds [5]) the superconducting copper-oxide layers are separated by several insulating layers. The superconducting properties perpendicular to the layers are therefore best understood in terms of Josephson tunneling. Consequently, the topological defects in these materials are Josephson vortices instead of the Abrikosov vortices known from conventional type II superconductors. An understanding of the properties of the quasi two dimensional materials is therefore closely linked to an understanding of the dynamics of Josephson vortices.

In this Letter we take a closer look at a simplified system where Josephson vortices dominate the dynamics. The system mimics a situation where an incomplete copper-oxide layer forms an edge dislocation. Likewise the system

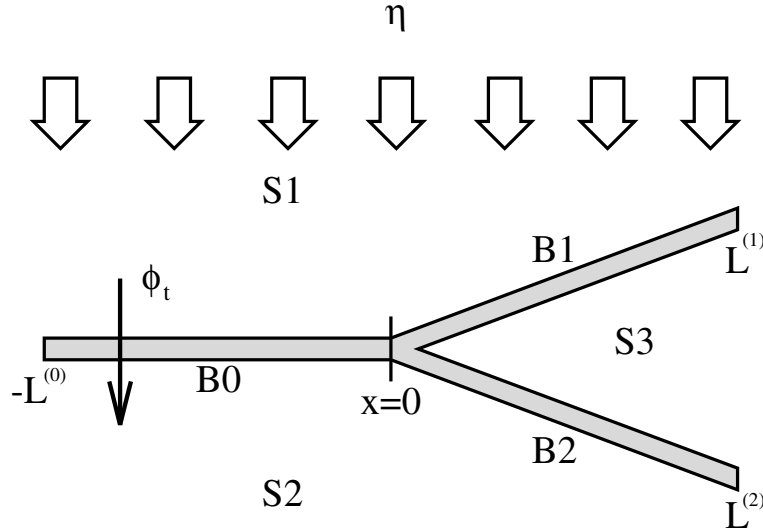


Fig. 1. Schematic diagram showing the system. The three superconductors S1, S2, and S3 are separated by an insulating barrier (grey) with three branches B0, B1 and B2. A current  $\eta$  is injected uniformly through the barrier. The voltage across the barrier is proportional to  $\phi_t$ . We define  $x$  positive to the right along the barrier, with origin at the branching point. The barrier forms three long Josephson junctions with lengths  $L^{(n)}$  in normalized units. S3 describes the extra superconducting layer wedged in between two layers to form an edge dislocation.

mimics a system of stacked Josephson transmission lines with an extra superconducting layer wedged into one of the barriers. This situation may be realized deliberately or accidentally during the preparation of the stacked system.

Our model is very simple: three Josephson transmission lines (long Josephson junctions (LJJ)) are coupled via a single common point (Fig. 1). Hence, if we think of an edge dislocation in a high temperature superconductor we have neglected the spatial dimension parallel to the defect, and second we have neglected all layers but the those forming the actual system. Furthermore, we neglect mutual interaction between Josephson currents flowing in different barriers. Thus, each of the three transmission lines is modeled by three perturbed sine-Gordon equations:

$$\phi_{xx}^{(n)} - \phi_{tt}^{(n)} - \sin(\phi^{(n)}) = -\eta + \alpha \phi_t^{(n)} \quad (1)$$

where upper indexes  $n = 0, 1, 2$  label the different branches of the system (B0, B1, and B2), and the lower indices specify partial differentiation with respect to the index. In these equations currents are normalized to the critical current, time to the inverse plasma frequency  $\omega_p^{-1}$  and lengths are normalized to the Josephson penetration depth  $\lambda_J$ .  $\eta$  is the current density supplied by an external circuit and  $\alpha$  is the normalized linear quasi particle conductivity.

In passing let us mention the single fluxon or  $2\pi$ -kink solution to the unperturbed Sine-Gordon equation (Eq. (1) without the right hand side):

$$\phi(x, t) = 4 \tan^{-1}(\exp(\pm \gamma(x - ut))) \quad (2)$$

where  $u$  is the velocity and  $\gamma(u) = (1 - u^2)^{-1/2}$ . In general when  $\phi_x(x, t)$  is positive we will call it a soliton (the plus in Eq. (2)) and an antisoliton for negative  $\phi_x(x, t)$  (the minus sign Eq. (2)). When the polarity is not important we use the term fluxon. Eq. (2) is the basis for much analysis [6], although it is not in general an exact solution to Eq. (1) and the boundary conditions (see below). The perturbation provided by  $\eta$  acts as a driving force to the fluxons: solitons in the negative  $x$  direction for  $\eta > 0$  and vice versa for antisolitons. The  $\alpha$  term acts as a damping force.

To completely specify the problem we need some boundary conditions [7]:

$$\phi^{(0)}(0) = \phi^{(1)}(0) + \phi^{(2)}(0) \quad (3)$$

$$\phi_x^{(0)}(0) = \phi_x^{(1)}(0) = \phi_x^{(2)}(0) \quad (4)$$

$$\phi_x^{(0)}(-L^{(0)}) = \phi_x^{(1)}(L^{(1)}) = \phi_x^{(2)}(L^{(2)}) = 0 \quad (5)$$

Eqs. (3) and (4) express that the voltage across the barrier and the surface current of the London layers respectively should be continuous across the branching point, whereas Eq. (5) expresses that surface currents at the ends should be zero. The latter is applicable when no external magnetic field is applied.  $L^{(n)}$  are the normalized lengths of the respective branches. In what follows we will assume  $L^{(0)} = L^{(1)} = L^{(2)} = L$ .

This model is a minimal model of an edge dislocation. All that remains of the properties of the original model is the branching point, where special boundary conditions apply. We present extensive simulations of the model and find very rich dynamics compared with a single LJJ.

This Letter is organized in the following way: In section 2 we will recall and re-discuss some results from our previous work [8], in section 3 we present the simulations of three types of periodic states, and in section 4 we briefly discuss the implications of our investigation and conclude.

## 2 Static states, oscillatory states and transient dynamics

The boundary conditions Eqs. (3) and (4) are what distinguishes our system from the usual long Josephson junction. It implies some special static properties which were discussed in some detail in Ref. [8] for the case  $\phi^{(1)}(x) =$

$\phi^{(2)}(x)$ . Let us briefly summarize the situation and present a few new results before discussing the fluxon dynamics in detail.

When  $\eta \neq 0$  and no fluxons are present the boundary conditions require, that  $|\phi^{(0)}(0)| > |\sin^{-1}(\eta)|$  and  $|\phi^{(1)}(0)| = |\phi^{(2)}(0)| < |\sin^{-1}(\eta)|$ , implying that some fraction of a flux quantum is trapped at the branching point. An approximate analytic expression for the background solution was given in Ref. [8]. The fractional flux leads to an instability when  $|\eta| > \eta_{gen} = 0.957$  where fluxon pairs are spontaneously created at the branching point. Hence, no static states can exist above this value, in contrast to a single LJJ where static states exist for  $|\eta| < 1$ . The value  $\eta_c = 0.957$  is therefore the true critical current of the system. For very strong damping ( $\alpha \gtrsim 0.5$ ) the spontaneous generation of fluxons may lead to a dynamics very similar to the Shapiro steps observed in LJJ in an applied external field. We will refer to this situation as the generating state.

The branching point acts via its boundary conditions as a pinning center for fluxons. Hence, a fluxon may be trapped at the branching point. For  $\eta = 0$  the solution is that of Eq. (2) (neglecting an unimportant mismatch in boundary conditions due to the finite length), but with a slice of the middle section cut away to match the boundary conditions at the branching point. The energy of the trapped fluxon is 6 in normalized units. This is to be compared with the energy 8 of a free static fluxon on an infinite line. A solution with two fluxons trapped (double fluxon) is unstable [8].

For  $\eta > 0$  a trapped soliton is dragged into B0, whereas an antisoliton is pushed towards B1 and B2. The situation is reversed for  $\eta < 0$ . When dragged into B0 the fluxon escapes when the threshold value  $|\eta| = \eta_- = 0.228$  is reached. When pushed towards B1 and B2 it escapes at the threshold value  $|\eta| = \eta_+ \approx 0.43$ , in contrast with the value 0.650 reported in Ref. [8]. The reason for the discrepancy is that the symmetry assumed in the previous work is spontaneously broken at the lower threshold value, and the fluxon escapes into either B1 or B2. We observed it in simulations without introducing any asymmetry or noise, except for the unavoidable "computational" noise. It is not unreasonable to assume that the caught fluxon solution becomes unstable as soon as  $|\phi^{(1)}(0)| = |\phi^{(2)}(0)| = \pi - \sin^{-1}(\eta)$ . Repeating the analysis of Ref. [8] with this restriction in mind we arrive at the value  $\eta_+ = 0.42856$ .

Linearizing the wave-equations Eq. (1) around the trapped fluxon solution ( $\Phi(x, t) = \Phi_{trapped}(x) + u(x, t)$ , and  $u(x, t) \ll 1$ ) for  $\alpha = 0$  one obtains an effective Schrödinger equation for small amplitude modes. One such oscillatory mode where the fluxon oscillates from B0 symmetrically into B1 and B2 and back was reported in Ref. [8]. For  $\eta = 0$  the frequency was found analytically. Another mode leading to *exactly* the same "quantum mechanical" problem for  $\eta = 0$  appears if one assumes an antisymmetric mode with  $u^{(0)} = 0$  in B0

and  $u^{(1)} = -u^{(2)}$  in B1 and B2. Hence, the two modes oscillate with the same frequency for  $\eta = 0$ , and a general oscillation will be a superposition of the two. When finite  $\eta$  is applied the effective potential will be different for the two modes, and they will be modified differently leading to a splitting of the frequencies. For instance, we know that the frequency of the antisymmetric mode vanishes, when  $\eta \rightarrow \eta_+$  leading to the spontaneously broken symmetry and fluxon escape discussed above, whereas the frequency of the symmetric mode will vanish only when  $\eta \rightarrow 0.650$ , the value found in Ref. [8].

Since the branching point acts as a pinning center an incoming fluxon may be trapped if its kinetic energy is below some threshold. If we assume that an incoming fluxon has already reached its equilibrium velocity determined by the balance between the driving force  $\eta$  and the damping provided by  $\alpha$  the kinetic energy is uniquely determined by the driving current. Thus there exists a threshold current  $\eta_0$  below which a fluxon entering from B0 is trapped, and a threshold  $\eta_{1,2}$  below which a fluxon entering from B1 or B2 is trapped.  $\eta_0$  and  $\eta_{1,2}$  were mapped in Ref. [8]. Notice that  $\eta_0$  was computed for a completely undisturbed system, and as such was completely symmetric with respect to B1 and B2. If the symmetry is broken by some disturbances it may happen that the incoming fluxon is guided into B1 or B2 without having to create two extra fluxons. In such cases  $\eta_0$  is not directly relevant.

So far we have only discussed the implications of the special boundary conditions at the branching point. The end points are very important as the fluxons may be reflected back into the branch (with opposite polarity) and thus allow for repetitive dynamics and stationary periodic states. However, if the kinetic energy is too low the fluxon will be annihilated due to enhanced damping during the reflection process [9]. Again, if we assume that the fluxons have reached their equilibrium velocity before the reflection, we can characterize the situation in terms of a threshold current  $\eta = \eta_{an}$  below which the fluxons annihilate at the end points. Hence, below  $\eta_{an}$  fluxons leave the system and will usually prevent the existence of periodic states (the exception is the “generating state” mentioned earlier). Notice that this is the only inherent mechanism which may change the net number of fluxons (number of solitons minus antisolitons) in the system.

The different threshold values are summarized in Fig. 2. In the region below  $\eta_{an}(\alpha)$  and  $\eta_{gen}$  no dynamical periodic states are possible. Below  $\eta_0$  periodic dynamical states involving only one fluxon will need some mechanism to guide the fluxon from B0 into B1 or B2 to survive. Similarly, above  $\eta_0$  a mechanism which prevents the creation of several fluxons at the branching point is necessary to preserve the one fluxon state. As one may imagine states relying on such delicate mechanisms have only a limited range of stability.

It is interesting to note that if one increases the current slowly (on the scale of

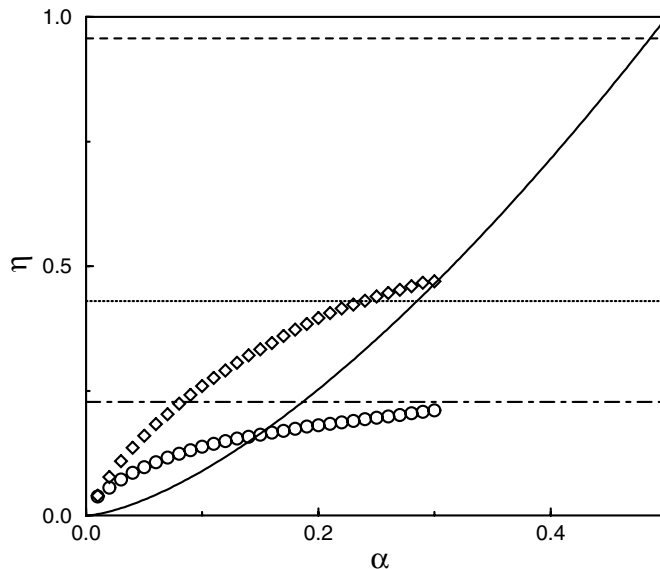


Fig. 2.  $\eta$ - $\alpha$ -diagram showing the different threshold values discussed in the text. Diamonds and circles are  $\eta_{1,2}(\alpha)$  and  $\eta_0(\alpha)$  (from Ref. 6). Full line is  $\eta_{an}(\alpha)$ , dash-dot line is  $\eta_- = 0.228$ , dotted line is  $\eta_+ = 0.43$  and the dashed line is  $\eta_{gen} = 0.957$ .

$\omega_J^{-1}$ ) with a fluxon trapped different situations occur depending on the value of  $\alpha$  as the current exceeds the threshold values discussed above. For instance, for a trapped fluxon escaping into B0 when  $|\eta| = \eta_-$  there are three different outcomes. If  $\alpha$  is such that  $\eta_-$  is above  $\eta_0$  the fluxon is first reflected at the end and then injects fluxons into B1 and B2 and one is reflected back into B0. This will inevitably lead to a dynamical state with the possibility of a periodic state. If, however,  $\eta_-$  is below  $\eta_0$  but above  $\eta_{an}$  the fluxon is reflected at the boundary, but only to be caught at the branching point. The state will then remain static until a further increase of the current beyond  $\eta_+$  allows the fluxon to escape into B1 or B2. Finally if  $\eta_-$  is below  $\eta_{an}$  the fluxon will annihilate with its mirror fluxon at the end and the system will remain empty and static until a further increase of the current beyond  $\eta_{gen}$  will start the spontaneous creation of fluxons.

### 3 Periodic states

We have found very rich dynamics of the system and many different dynamical states where the dynamics is repeated after some period  $T$ . We define the voltage  $v$  of a periodic state as:

$$v = \frac{1}{L^{(0)} + L^<} \left\{ \int_{-L^{(0)}}^0 \langle v^{(0)}(x) \rangle dx + \int_0^{L^<} [\langle v^{(1)}(x) \rangle + \langle v^{(2)}(x) \rangle] dx \right\} \quad (6)$$

where  $L^< = L^{(1)} = L^{(2)}$  and we have allowed for different lengths  $L^{(0)} \neq L^<$ . Here we have introduced the average voltages over one period:  $\langle v^{(n)}(x) \rangle = T^{-1} \int_t^{t+T} \phi_t^{(n)}(x, t) dt = T^{-1} [\phi^{(n)}(x, t+T) - \phi^{(n)}(x, t)] = 2\pi m^{(n)} T^{-1}$ , where  $m^{(n)}$  are integers. Boundary conditions require that  $m^{(0)} = m^{(1)} + m^{(2)}$ . Notice that the voltages of B1 and B2 are summed to give the total voltage across the system along those branches.

In a fluxon state the phase in an arbitrary point is only changed by  $2\pi$  every time a fluxon passes, and since the velocity of fluxons is limited by the speed of light ( $= 1$ ) the voltage of a fluxon state is limited by the number of fluxons and the length of the system. This gives rise to the very characteristic steep  $\eta - v$  curves known as zero field steps (ZFS). They are for convenience labeled by the number of fluxons, eg. ZFS14.

### 3.1 Rotating states

The simplest dynamical states are the ones containing no fluxons (referred to as rotating solutions), and are characterized by almost linearly growing (or decreasing) phases in each point of the junctions. For a single LJJ one would only find one rotating state, where each point of the junction roughly behaves as a small Josephson junction ( $\phi_x = 0$  everywhere). For our system, however, there are two distinct states: one where all branches rotate (are in their normal state as opposed to the superconducting state), and one where B1 or B2 is static. The latter can only exist for  $|\eta| < 1$ , since in the static branch  $\langle \phi \rangle = \sin^{-1} \eta$ . Assuming that in the dynamical branches  $\phi^{(n)}(x, t) \approx \omega_- t + c^{(n)}$  where  $c^{(n)}$  are constants, we find by substitution into Eq. (1):

$$v_{rot-} = \omega_- = \frac{\eta}{\alpha} \quad (\text{one static branch}) \quad (7)$$

Boundary conditions require that  $c^{(0)} - c^{(1,2)} = \sin^{-1} \eta$ .

For  $|\eta| > 1$  the *only possible* state is the one with all branches rotating, but its range of stability will usually extend into  $|\eta| < 1$ . Each of the branches would—if they were not connected at the branching point—rotate with the frequency  $\omega_-$ , but the boundary conditions at the branching point require that  $\omega^{(0)} = \omega^{(1)} + \omega^{(2)} = 2\omega^{(1,2)}$ . Neglecting oscillating terms we assume that  $\phi^{(n)}(x, t) = \omega^{(n)} t + u^{(n)}(x)$ . Substituting into Eq. (1) again we find:

$$v_{rot+} = \omega^{(0)} = 2\omega^{(1,2)} = \frac{2(L^{(0)} + L^<)}{2L^{(0)} + L^<} \frac{\eta}{\alpha} \quad (\text{all branches rotating}) \quad (8)$$

Due to the branching point B1 and B2 are forced to rotate with a slower frequency, and B0 with a higher frequency than a single LJJ. Hence, the excess power supplied by  $\eta$  in B1 and B2 is transferred into B0 where it is extracted by the  $\alpha$  term.

The voltage of the two rotating solutions obtained from simulations with  $L^{(0)} = L^{(1)} = L^{(2)} = 10$  are plotted in Fig. 3 as crosses. There is no noticeable deviation from straight lines confirming the validity of Eqs. 7 and 8. The full range of stability as found in the simulations is plotted. Notice that the  $v_{rot-}$  curve is disconnected due to instability near ZFS's (discussed below).

### 3.2 Fluxon states

The system shows a remarkable variety of fluxon states, and before discussing them in detail we will introduce some notation. To describe the dynamics of one period of a state in detail we usually just need to specify the path of each fluxon. We will use the notation (01) to describe a state containing one fluxon which repeatedly is in B0, enters B1 and goes back into B0. The sequence (0102) would then describe a similar state but where the fluxon every second time enters B1 and B2 when approaching the branching point. If more than one fluxon is involved we specify sequences separated for all fluxons separated by commas. In this case it is important to correlate the order of the different sequences. For instance a two fluxon state could be described as (01,10) and another one as (01,01). The former would describe a state where the fluxons exactly swap places at the branching point, and the latter a state where the two fluxons were moving in a train, thus entering the two branches simultaneously. If a fluxon is trapped at the branching point we will specify a # instead of the branch number.

For states with many fluxons the introduced notation is cumbersome and it is often impossible to identify the path of each and every fluxon. In such cases we have usually found a constant number of fluxons in each branch at any time allowing us to simply specify the number of fluxons like  $\{10, 8, 2\}$  for a state with ten fluxons in B0, eight fluxons in B1, and two fluxons in B2.

In order to use simulations to look at the many dynamic states we employed a computer program using a finite difference method to solve the partial differential equations Eq. 1. During the simulations the  $\phi(x, t)$  profiles were mapped directly to the screen in real time. This allowed us to interactively change the applied current  $\eta$  smoothly at least on a time scale comparable to  $\omega_J$ , and then fix the current to see what solution evolves. In experiments the current is usually changed over time scales orders of magnitude higher. Our simulations resemble the experiment as much as possible though. During the simulations

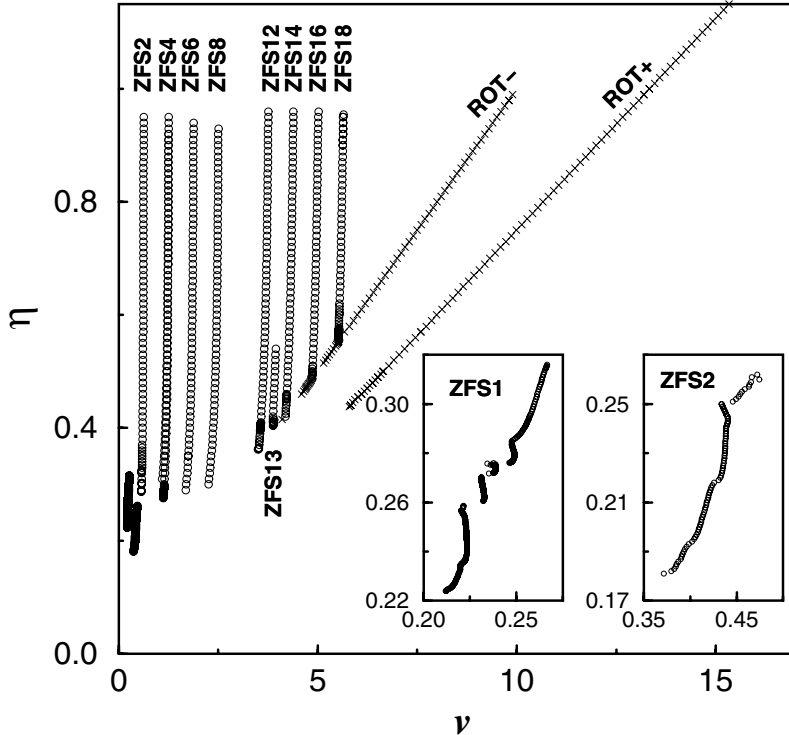


Fig. 3. Simulated  $\eta - v$  curves (IV characteristics) showing the two linear rotating states (crosses) and several zero field steps (circles). The insets show ZFS1 and details of ZFS2.  $L^{(0)} = L^{(1)} = L^{(2)} = 10$  and  $\alpha = 0.1$ .

we could introduce new fluxons in each of the branches by twisting the phase at the end points by  $2\pi$ . In this way it was easy to generate new solutions, and investigate their stability. For all the simulations we show here we have fixed  $\alpha = 0.1$  and  $L^{(0)} = L^{(1)} = L^{(2)} = 10$ .

The output from the simulations is an  $\eta - v$  characteristic. The result of our efforts is summarized in Fig. 3. The figure contains the voltage and current for all the periodic states we have been able to find. In some cases we found states which seemed stable during our time of observation (typically thousands of normalized time units) but did not show strict periodicity as is needed for the computer program to calculate the voltage. Such states are not represented in the figure.

There are two main regimes for the periodic states: a low current regime and a high current regime. The boundary between the two regimes is *roughly* given by the threshold for capture of fluxons coming from B0.

### 3.2.1 Low current regime

At first sight the simplest periodic fluxon state should contain only one fluxon. There are, however, several difficulties which tend to inhibit such a state. First of all when a fluxon hits the branching point from B0 it will either be trapped or it will penetrate into the other branches. Obviously if the fluxon is trapped it is not a periodic state. With  $\alpha = 0.1$  the threshold is approximately  $|\eta| \approx 0.27$ . On the other hand, if the fluxon is not trapped it will usually for symmetry reasons create fluxons in B1 and B2 and an antifluxon in B0. The three fluxons are reflected at the end points and returns to the branching point almost simultaneously. Ideally they could annihilate into a single fluxon traveling back into B0, but usually they continue to create more and more fluxons until a steady state is reached. Thus to sustain a single fluxon periodic state it is necessary to break the symmetry when the fluxon hits the branching point. It turns out that there are in fact periodic states where the fluxon is guided into B1 or B2. Since the empty state has no bound oscillations—as for the captured fluxon—the guiding mechanism must be provided by plasma waves excited every time the fluxon passes the branching point and traveling down the empty branches. Such a guiding mechanism is very subtle, and we find indeed that the stability of the one fluxon periodic states is rather limited. ZFS1 is shown in the left inset of Fig. 3. The step shows a complicated structure due to the dependence of the fluxon velocity on the driving current. Since the fluxon has to lock to the frequency of the plasma waves it is not surprising that the average velocity has a complicated  $\eta$ -dependence. The step is broken up into disconnected branches and parts of it has even negative slope. Between the branches the guiding mechanism breaks down and the fluxon is trapped at the branching point or more and more fluxons are created at the branching point. Along ZFS1 there are different states. Most often is it an (01) state, where the fluxon is guided into the same branch every time it approaches the branching point. In the topmost branch of ZFS1 it is an (0102) state where the fluxon switches between B1 and B2 every second time it approaches the branching point. In principle any sequence of switching into B1 and B2 is possible, and it is quite possible that there are more complicated patterns like (010102) etc. although we have not observed any stable states with complicated sequences.

In principle one could roughly think of any fluxon state as a superposition of single fluxon states, but the idea is not fruitful because of the subtle switching mechanism necessary to sustain the single fluxon states. The picture cannot explain the extended stability range for even number fluxon states and the almost complete absence of odd number fluxon states in our simulations. A better picture is provided below by the two fluxon states.

Another exotic low current state was found where an incoming fluxon from B0 is trapped at the branching point (Fig. 4). The state contains two fluxons at all times. When the two are in B0 the first one is trapped at the branching

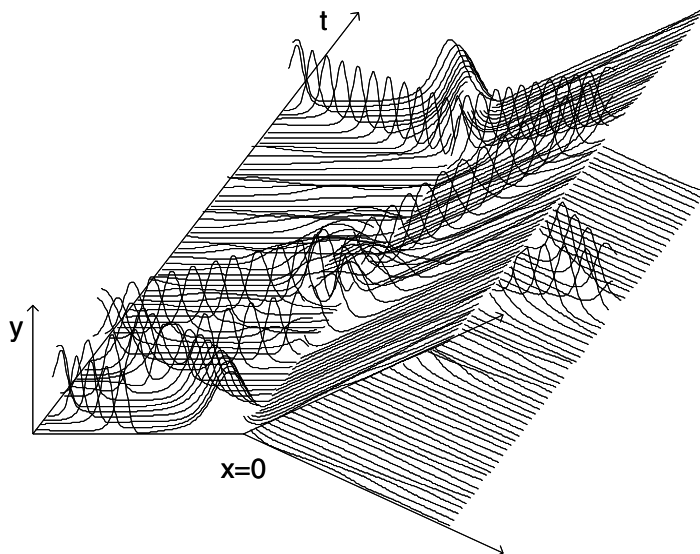


Fig. 4. Two fluxon state where one fluxon is trapped until the next fluxon arrives at the branching point. Spatial axes are arranged as in Fig. 1. Time axis points into the paper.  $y = 1 - \cos(\phi(x, t))$  is shown on the vertical axis.  $\eta = 0.19$ .

point until the second catches up with it. Then they create a “virtual” trapped double fluxon (which is unstable), and rapidly decays into two fluxons moving symmetrically into B1 and B2. The very strict symmetry leads us to use the term “virtual” since clearly the trapped fluxon is not first pushed into B1 or B2 before the next passes the branching point. When the two reflected fluxons return to the branching point they again become a “virtual” trapped double fluxon which even more rapidly decays into two separate fluxons. One is rapidly leaving the branching point while the second is held back for a while by the pinning force of the branching point and the repulsion from the first fluxon. When the two fluxons are reflected at the end point the pattern is repeated. The zero field step has again a complicated structure as shown in the right inset of Fig. 3. It reflects a complicated dependence of the decay rate of the “virtual” double fluxons on the applied  $\eta$ . In this case the state does not rely on a subtle switching mechanism since there is perfect symmetry between B1 and B2, and the step consists of one single branch. In our notation we may write this state as  $(01\#0, \#200)$ .

A similar state containing four fluxons was observed, and is essentially the superposition of two of the just mentioned states. The range of stability for this state was very limited. In general all the low current periodic states show very complicated structure of the zero field step and have a small range of stability. There is bound to be more periodic states than we have discussed here and with increasing complexity. The existence of periodic states where fluxons are created and annihilated at the branching point on a regular basis is

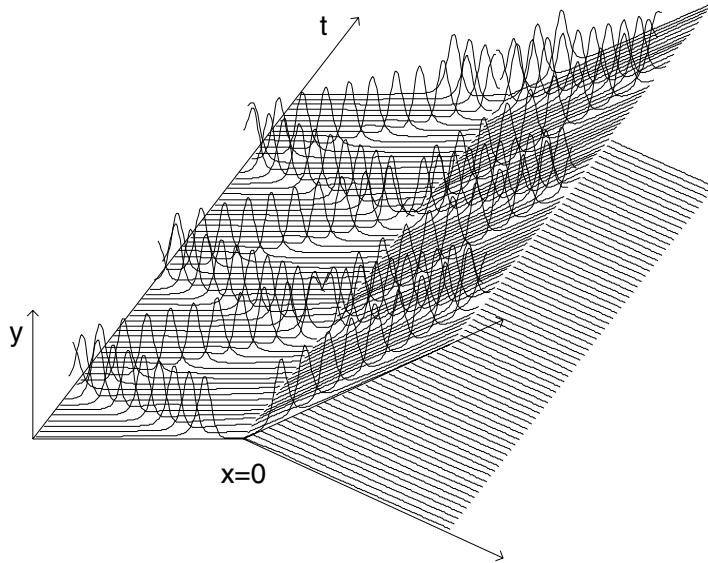


Fig. 5. The elementary two fluxon state which is the building brick for all even numbered fluxon states at high currents. Spatial axes are arranged as in Fig. 1. Time axis points into the paper.  $y = 1 - \cos(\phi(x, t))$  is shown on the vertical axis.  $\eta = 0.34$ .

possible, although the candidates found during our simulations always turned out to be unstable.

### 3.2.2 High current periodic states

It turns out that the elementary building stone which allows us to understand most of the higher zero field steps is a two fluxon periodic state (Fig. 5). In this state there is constantly a fluxon in B0 and one in B1 (or B2). The dynamics of the two fluxons is locked in such a way that they always meet at the branching point, where they swap branches or equivalently are reflected as if it was an end point. The locking ensures that  $\phi_x(0) \approx 0$  (it cannot be strictly zero when  $|\eta| \neq 0$  because of the background solution). This periodic state (in our notation  $(01, 10)$  and  $\{1, 0, 1\}$ ) yields ZFS2 and has a large stability range as is obvious from Fig. 3. In the figure is also displayed several even numbered zero field steps with large ranges of stability. All these ZFS can be visualized as a superposition of several two fluxon states. Since the choice of B1 or B2 for one of the fluxons is arbitrary for the two fluxon state, the even numbered fluxon states can be different combinations of these. Hence, an even  $2n$  fluxon state may in general be written as an  $\{n, m, n - m\}$  state with  $0 \leq m \leq n$ . In addition to this multitude of possibilities the order in which the fluxons in B1 and B2 are paired with those in B0 is arbitrary. It is likely, though, that states where the fluxons in B1 and B2 are spread evenly to minimize

the repulsion energy are most stable. In Fig. 3 there are two almost identical branches of ZFS4 corresponding to two such equivalent states (  $\{2, 1, 1\}$  and  $\{2, 0, 2\}$  ). For all the other numbers of fluxons only the ZFS corresponding to one solution has been traced out.

The reader may have noticed that a ZFS10 is absent from Fig. 3. We have not been able to generate a ten fluxon solution. ZFS2–ZFS8 were generated by introducing fluxons into the the ends of the branches by hand, whereas ZFS12–ZFS18 were spontaneously generated from the rotating solutions. None of these techniques led to a ten fluxon solution. We consider this a technical difficulty and the absence of a ZFS10 in our simulations is without significance.

Not all periodic states can be described as superpositions of ZFS2 states. We have for instance also found a state with thirteen fluxons shared between B0 and B1 with B2 empty (ZFS13, in our notation best described as  $\{6.5, 6.5, 0\}$ ). In this case the branching point continuously contains a fluxon passing from one branch to another. This causes radiation of rather high amplitude waves down the empty branch, and it leads to the smaller range of stability as observed in Fig. 3.

### *3.2.3 Discussion of fluxon dynamics*

For a more realistic system with arbitrary ratio between the lengths of the branches the picture is of course changed from the one just outlined, but the main features will persist. For the low current states it will probably lead to even less stability, and for the high current steps it will probably lead to a different set of “magic numbers” than merely the even numbered zero field steps. For the normal states we have already given a formula for the resistance in the general case.

We have not addressed the possibility of non-periodic states at all, and it is likely that some regimes will have such exotic dynamics, despite the absence of an external periodic reference signal.

In the context of edge dislocations we have not addressed the question of coupling between currents in the two parallel branches. Such interaction will tend to stabilize specific classes of states depending on the nature of the coupling, but will not alter the picture qualitatively.

## 4 Conclusion

We have found an enormous variety of dynamics in our simulations, which we may divide into three categories: the low current zero field steps, high current zero field steps and the rotating states.

In the low current steps the pinning force of the branching point is very significant and leaves the periodic states very vulnerable, since the dynamics depend on a subtle switching mechanism which serves to guide the fluxons into the two parallel branches. Therefore the zero field steps have very complicated structure containing negative slope regions.

For the high current steps (currents roughly above the threshold for fluxon capture) the major effect of the branching point is to virtually exclude the possibility of odd numbered zero field steps. Most of the high current steps may be viewed as superpositions of two fluxon states.

For currents lower than the critical current there are two “normal states” with different resistance. In the high resistance state all three branches are in their normal state, and the resistance is higher than for a single Josephson transmission line. In the low resistance state one of the parallel branches is in the superconducting state. In this case the resistance is equal to that of a single Josephson transmission line.

## 5 Acknowledgments

SAH would like to thank Carlsbergfondet for financial support.

## References

- [1] S. Sakai, P. Bodin, N. F. Pedersen, *J. Appl. Phys.* **73**, 2411 (1993); A. Ustinov, H. Kohlstedt, M. Cirillo, N. F. Pedersen, G. Hallmans, *Phys. Rev.* **B 48**, 10614 (1993); S. Sakai, A. V. Ustinov, H. Kohlstedt, A. Petraglia, N. F. Pedersen, *Phys. Rev.* **B 50**, 12905 (1994); T. Holst, J. Bindslev Hansen, N. Grønbech-Jensen, J. A. Blackburn, *Phys. Rev.* **B 42**, 127 (1990); N. Grønbech-Jensen, J. A. Blackburn, *Journ. Appl. Phys.* **74**, 6432 (1993); N. Grønbech-Jensen, D. Cai, A. R. Bishop, A. W. G. Lau, P. S. Lomdahl, *Phys. Rev.* **B 50**, 6352 (1994);
- [2] N. Grønbech-Jensen, P. S. Lomdahl, M. R. Samuelsen, *Phys. Rev.* **B 48**, 6353 (1993)

- [3] W. E. Lawrence, S. Doniach, *Proceedings of the Twelfth International Conference on Low Temperature Physics*, edited by E. Kanda (Academic Press of Japan, Kyoto 1971) 361.
- [4] L. N. Bulaevskii, M. Zamora, D. Baeriswyl, H. Beck, J. R. Clem, Phys. Rev. **B 50**, 12831 (1994)
- [5] R. Kleiner, P. Müller, Phys. Rev. **B 49**, 1327 (1994); N. E. Hussey, A. Carrington, J. R. Cooper, D. C. Sinclair, Phys. Rev. **B 50**, 13073 (1994).
- [6] D. W. McLaughlin, A. C. Scott, Phys. Rev. B **18**, 1652 (1978)
- [7] K. Nakajima, Y. Onodera, Y. Ogawa, J. Appl. Phys. **47**, 1620 (1976).
- [8] A. Grunnet-Jepsen, F. N. Fahrenndorf, S. A. Hattel, N. Grønbech-Jensen, M. R. Samuelsen, Phys. Lett **A 175**, 116 (1993)
- [9] N. F. Pedersen, M. R. Samuelsen, D. Welner, Phys. Rev. B **43**, 4057 (1984)